Journal of Catalysis **185,** 314–323 (1999)
Article ID jcat.1999.2521, available online at http://www.idealibrary.com on IDEAL®

Characterization of Ni/SiO_2 Catalysts Prepared by Successive Deposition and Reduction of Ni^{2+} Ions

K. Hadjiivanov,*,[1] M. Mihaylov,* D. Klissurski,* P. Stefanov,* N. Abadjieva,* E. Vassileva,† and L. Mintchev‡

*Institute of General and Inorganic Chemistry, Bulgarian Academy of Sciences, Sofia 1113, Bulgaria; †Faculty of Chemistry, University of Sofia, Sofia 1126, Bulgaria; and ‡Institute of Catalysis, Bulgarian Academy of Sciences, Sofia 1113, Bulgaria

Received September 30, 1998; revised April 12, 1999; accepted April 12, 1999

Different Ni/SiO_2 specimens have been synthesized by impregnation (sample Ni–*i*–Si) and grafting Ni^{2+} ions from nickel amminocomplex solution on (i) SiO_2 (sample Ni–1–Si) and (ii) reduced Ni–1–Si (sample Ni–2–Si). They have been characterized by TPR, IR spectroscopy, DR UV–VIS spectroscopy, XPS, XRD, TEM, and FMR. Due to the formation of surface silicates, the Ni^{2+} ions from Ni–1–Si exhibits low acidity and forms carbonyls only at low temperatures. They are characterized by a higher reduction temperature (TPR peak at 956 K) than the Ni^{2+} ions from the Ni–*i*–Si sample (two TPR peaks at 652 and 710 K). Highly dispersed metal particles are formed after reduction of the Ni–1–Si sample (ca. 2 nm in diameter), the CO adsorption reveals the lack of dense crystal planes. The reduced Ni–*i*–Si sample is characterized by a lower dispersion of nickel (main diameter of the metal particles of 16 nm). Exposure of the reduced Ni–1–Si sample to oxygen causes oxidation of all of the surface situated metal nickel to Ni^{2+}. These Ni^{2+} ions are reduced much more easily (TPR peak at 489 K) than those initially deposited. Part of the silica surface is regenerated during the reduction of nickel and is not blocked again after oxidation, which allows subsequent deposition of Ni^{2+} ions on the reduced catalysts. As a result, the nickel concentration increases. Reduced Ni–2–Si sample is also characterized by small nickel particles (ca. 2–3 nm in diameter). The results evidence that subsequent deposition–reduction of Ni^{2+} ions on silica can be used to prepare highly dispersed nickel catalysts with different nickel concentration.

1. INTRODUCTION

The synthesis of supported metal catalysts is generally aimed at reaching maximum dispersion of the metal with a view to its more efficient participation in the catalytic processes. However, for a number of reactions (the so-called structure sensitive reactions) the catalytic activity depends on the metal particle size, sometimes passing through a maximum (1). The data for the structure-sensitive reactions are often scarce because of the lack of appropriate samples with well defined monodisperse metal particles. For that reason, it is of definite interest to develop reliable methods for synthesis of supported metal catalysts, which are characterized, in the ideal case, by a predetermined diameter and a narrow metal particle size distribution. This would allow obtaining new data on the structure-sensitive reactions and thus development of more effective catalysts.

The mean diameter of supported metal particles depends on different factors, including synthesis method (1–11), kind of the support (1–4, 12, 13), concentration of the metal (1, 12), prereduction treatment (1, 14), and reduction conditions (1, 12, 15). Impregnation is the most widely applied technique for preparation of supported catalysts. This method, however, often leads to inhomogeneous distribution of the active phase and to its low dispersion. Techniques usually ensuring the formation of highly dispersed metal catalysts are ion-exchange, deposition–precipitation, and coprecipitation (1–11). The so-called ion exchange occurs only when there is specific interaction between the metal ions and the support (1–8). This method has restricted possibilities of controlling the active phase content: the uptake coverage is limited by the number of active sites for exchange.

By studying the mechanism of photocatalytic silver deposition on titania (16) we established that the reduction of the adsorbed Ag^+ ions leads to regeneration of the sites when the silver has been initially located. This phenomenon has been the basis for proposing, a few years ago, a new method for the synthesis of supported metal catalysts, namely multiple ion-exchange (6). The metal ions are deposited by ion-exchange and then reduced. During the reduction a large fraction of the original sites for exchange are liberated. This allows subjecting the reduced catalyst to a second ion-exchange, etc. The method combines some of the advantages of the ion-exchange (e.g., homogeneous distribution of the active phase and formation of high-dispersion metal) with the possibility of synthesizing catalysts with a higher metal concentration. The multiple ion-exchange has been applied successfully to the Pt/TiO_2 system and resulted in formation of well defined platinum particles with a narrow particle size distribution (6). It has been established, however, that the process is not a real ion-exchange, but rather

[1] To whom correspondence should be addressed.

0021-9517/99 $30.00

adsorption of cations on titania, which results in blocking of the Lewis acid sites. For that reason, we have proposed that a more informative way of denoting the technique is successive adsorption and reduction (17), or more generally, successive deposition–reduction (SDR).

Deposition of nickel by SDR could meet some difficulties. Supported nickel catalysts are often oxidized in air (12) which might lead to a redistribution of nickel onto the support surface, and thus the next deposition might be hindered. We have studied the possibility of applying SDR to prepare titania- (17) and zirconia-supported (18) nickel. In both cases SDR led to an increase in nickel concentration. However, the SMSI affected the processes and the resulting metal particles were of low dispersion (about 20 nm in diameter for the Ni/TiO_2 system). No SMSI is typical with silica (19). In addition, silica, compared to other supports, usually ensures a better dispersion of nickel, irrespective of the preparation method (12). For these reasons we tried to establish the applicability of SDR for synthesis of Ni/SiO_2 catalysts. Ni/SiO_2 samples have been prepared by SDR and have been characterized by different techniques. A sample prepared by impregnation was also studied for the sake of comparison. It was demonstrated that, here again, no real ion-exchange occurs and the process is better described by the term successive deposition–reduction.

2. EXPERIMENTAL

2.1. Catalyst Preparation

The silica support used was a commercial Aerosil sample with a specific surface area of 336 $m^2\ g^{-1}$.

Two different methods were applied to the preparation of the Ni/SiO_2 catalysts: deposition of Ni^{2+} ions by grafting from nickel amminocomplex solution (including SDR) and impregnation. Some characteristics of the Ni/SiO_2 samples studied, as well as the notations that will be used further on in the text, are presented in Table 1.

To prepare Ni–1–Si, 10 g of SiO_2 was suspended in 150 ml 0.1 M Ni^{2+} solution obtained from $Ni(NO_3)_2$ and containing 12.5 wt% ammonia (pH 12.3). The mixture was agitated for 1 h and then the precipitate was filtered, washed thoroughly with water, and dried. Finally, the sample was calcined for 1 h at 623 K in order to remove adsorbed ammonium ions.

TABLE 1

Some Characteristics of the Ni/SiO_2 Samples Studied

Notation	Preparation technique	Concentration of Ni (wt%)
Ni–*i*–Si	Impregnation of SiO_2 by $Ni(NO_3)_2$ solution	1.70
Ni–1–Si	Grafting Ni^{2+} on SiO_2 from $Ni^{2+}(NH_3)_x$ solution	1.72
Ni–2–Si	Second deposition of Ni^{2+} on reduced Ni–1–Si	2.63
Ni–3–Si	Third deposition of Ni^{2+} on reduced Ni–2–Si	3.31

Ni–2–Si was prepared in the same way, but in this case the reduced Ni–1–Si sample was utilized instead of the pure support. All the other procedures were as described above for the preparation of the Ni–1–Si sample. Analogous were the procedures for the third deposition.

Ni–*i*–Si was synthesized by incipient wetness impregnation of silica with a nickel nitrate solution. In order to decompose the nickel nitrate completely, the catalyst was calcined for 1 h at 723 K. The nominal nickel concentration was calculated in such a way that it corresponded to the concentration in the Ni–1–Si catalyst.

All samples were reduced in a flow of 10 vol% H_2 in Ar with a flow rate of 50 ml min^{-1}. The samples were exposed to this flow at ambient temperature, while the reduction temperature (TR) was attained with a heating rate of 5 K min^{-1}. After 1 h reduction at TR the samples were cooled to room temperature in argon. The TR for all Ni/SiO_2 specimens prepared by deposition from nickel amminocomplex solution was 973 K, whereas for Ni–*i*–Si it was 773 K.

2.2. Apparatus

The TPR experiments were performed with 10 vol% hydrogen in argon (30 ml min^{-1}) at a heating rate of 10 K min^{-1}, the hydrogen consumption being measured by a catharometric detector. All TPR profiles were normalized for the same catalyst mass.

The IR spectra were recorded by a Bruker IFS-66 apparatus at a spectral resolution of 1 cm^{-1} accumulating 128 scans. The *in situ* IR cell was connected to a vacuum/sorption system with a residual pressure less than 10^{-3} Pa. The specially constructed cell allowed the IR measurements to be performed between 85 K and ambient temperature. Prior to the experiments, the samples were pressed into self-supporting pellets and heated directly in a vacuum–absorption apparatus. The activation was carried out by successive thermooxidative (1 h, 20 kPa oxygen) and thermovacuum (1 h) treatments at 673 K.

The XPS measurements were performed by an ESCALAB Mk II (VG Scientific) apparatus with a magnesium anode ($h\nu = 1254.6$ eV). The binding energy values were corrected using the C 1*s* level (284.8 eV) of the carbon contaminants on the surface.

The diffuse reflectance UV–VIS spectra were recorded by a Beckman 5270 UV–VIS spectrometer utilizing $BaSO_4$ as white standard.

The X-ray phase analysis was made by a DRON-3 apparatus with a CuK_α radiation source.

The electron microphotographs were taken by a JEOL JEM 100B transmission electron microscope with an 80-kV accelerating voltage.

The FMR measurements were performed with a PS 100X CentroSpectr (Minsk) spectrometer using 100 kHz modulation of the magnetic field. The *g* values were determined with respect to DPPH.

The nickel content of the catalysts was determined by flame atomic absorption spectrometry at the resonance wavelength using a PYE-UNICAM SP 1950 apparatus.

3. RESULTS

3.1. Temperature-Programmed Reduction

TPR is a favorable technique for studying supported nickel catalysts. Bulk NiO is characterized by a TPR peak at 673 K (20), whereas when the nickel ions interact with the supports (e.g., forming surface compounds) their reduction temperature considerably increases (10, 20, 21). A "NiO"-like defect phase, produced by oxidation of supported metal nickel, is reduced in the temperature interval of 383–628 K: the higher the temperature of preliminary calcination, the higher the reduction temperature (14, 20).

The TPR profiles of our Ni/SiO_2 samples are shown in Fig. 1. The impregnated Ni–*i*–Si catalyst produces an asymmetric peak consisting of two components with maxima at 652 and 710 K (Fig. 1, curve a). This evidences some inhomogeneity of supported nickel. According to data from the literature (4, 8–10, 13, 22–24), the TPR peaks are due to reduction of the supported "NiO"-like phase.

The TPR profile of sample Ni–1–Si displays a broad peak with a maximum at 956 K (Fig. 1, curve b) which can be ascribed to reduction of Ni^{2+} ions from surface nickel philosilicates to metal nickel (4, 8–11, 13, 22, 24). After the TPR procedure, the sample has been contacted with air at ambient temperature for 1 h. The properties of this reoxidized Ni–1–Si strongly differ from those of the fresh sample: the TPR pattern contains a peak with a maximum at 489 K; i.e., the reduction temperature is by about 470 K lower (Fig. 1, curve c). These results evidence that, regardless of the fact that exposing a reduced sample to air leads to oxidation of part of the nickel, the oxidized phase obtained differs very much in properties from the nickel-containing phase in the fresh sample.

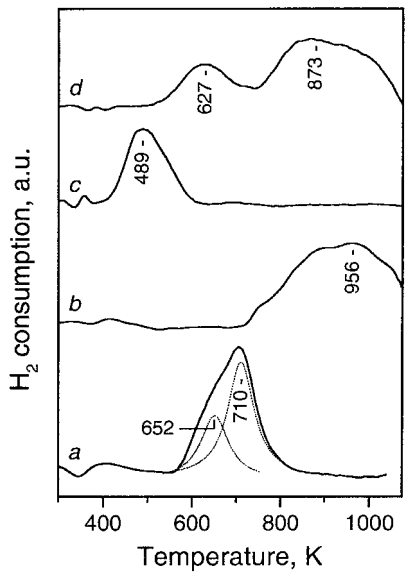

FIG. 1. TPR profiles of Ni–*i*–Si (a), Ni–1–Si (b), Ni–1–Si subjected to TPR and reoxidized in air at 293 K (c), and Ni–2–Si (d).

The TPR profile of Ni–2–Si shows two peaks with maxima at 627 and 873 K (Fig. 1, curve d). The high-temperature peak resembles in shape and position the peak for Ni–1–Si and can be attributed to reduction of nickel ions from surface nickel silicates. The presence of the low-temperature peak evidences the inhomogeneity of nickel in this sample. This peak can be assigned to reduction of reoxidized nickel ions originating from the first deposition. It should be noted that the maximum is at a higher temperature than the maximum of the peak detected with reoxidized Ni–1–Si. This seems to represent a contradiction, but is in fact due to the different reoxidation temperatures: before the TPR the Ni–2–Si sample has been calcined at 623 K.

3.2. Infrared Spectroscopy

Infrared spectroscopy of probe molecules has been used to estimate the state of nickel in the samples. Carbon monoxide is a probe molecule which allows separate monitoring of Ni^{2+}, Ni^{+}, and Ni^{0} on the surface of supported nickel catalysts. Carbonyls of the Ni^{2+}–CO type are detected only under equilibrium pressures and produce bands at 2220–2180 cm^{-1} (3, 25–30). With Ni^{+} ions carbon monoxide forms stable monocarbonyls (2160–2110 cm^{-1}) (26–29), which may be converted into dicarbonyls (ν_s(CO) at 2145–2131 cm^{-1} and ν_{as}(CO) at 2100–2081 cm^{-1}) (26, 27) under equilibrium CO pressures. The typical bands for linear carbonyls of metal nickel are observed at about 2060 cm^{-1}, whereas the bridged nickel carbonyls are visible below 2000 cm^{-1} (3, 26, 29–32). In addition, bands due to $Ni(CO)_x$ species can be detected below 2130 cm^{-1} (17, 18, 33, 34).

The IR spectrum of activated Ni–1–Si is essentially the same as those observed with pure silica. It exhibits three broad bands within the 2000–1600 cm^{-1} region which characterize overtones of lattice vibrations (1990 and 1626 cm^{-1}) and a combination frequency (1872 cm^{-1}) (35). Own absorption of the sample determines the so-called "cut-off" at about 1350 cm^{-1}: below this frequency the sample is opaque and no spectra of surface compounds can be detected there. In the region of the OH stretching modes there is a narrow band with a maximum at 3742 cm^{-1} which characterizes terminal groups of the Si–OH type.

The introduction of CO (1.6 kPa) to the Ni–1–Si sample produces no CO bands. This indicates that either nickel has penetrated in the catalyst bulk or Ni^{2+} ions are present on the surface but possess a very weak electrophilicity. The

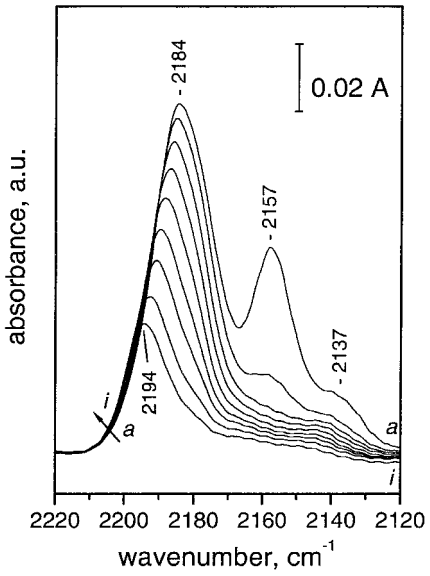

FIG. 2. FTIR spectra of CO adsorbed on Ni–1–Si at 85 K. Equilibrium CO pressure of 10 Pa (a) and evolution of the spectra under dynamic vacuum (b–i).

existence of surface Ni^+ ions or Ni^0 atoms can be excluded because in both cases carbonyl complexes should be formed and detected (26–30).

Adsorption is favored at low temperatures and species that are not stable at room temperature can thus be detected. In order to establish whether Ni^{2+} ions are present on the Ni–1–Si surface, we have studied the adsorption of CO at 85 K. Introduction of CO (10 Pa equilibrium pressure) at 85 K to the sample leads to the appearance of three principal bands in the IR spectrum, their maxima being at 2184, 2157, and 2137 cm^{-1} (Fig. 2, spectrum a). The band at 2137 cm^{-1} is typical of physically adsorbed CO and disappears easily upon evacuation (Fig. 2, spectra b–i). The next band that vanishes with pumping is that at 2157 cm^{-1}. Its intensity changes simultaneously with the red shift of the 3742 cm^{-1} Si–OH band by −93 cm^{-1}. This behavior is typical of the silanol groups on pure silica where the same shift of the OH stretches has been detected upon low-temperature CO adsorption (36). Thus, the 2157 cm^{-1} band is assigned to H-bonded CO. The band at 2184 cm^{-1} has not been observed with silica and is thus attributed to CO polarized by Ni^{2+} ions (3, 25–30). This band decreases in intensity during evacuation and its maximum gradually shifts to higher frequencies. Even after 10 min evacuation at 85 K, however, the band keeps a significant part of its intensity.

To develop an easier way of detecting surface Ni^{2+} ions with a low acidity we also studied the adsorption of NO. Nitrogen oxide is a little stronger base than CO and thus cations, that are inert toward CO adsorption at room temperature, may be monitored by NO. With supported Ni^{2+} cations NO forms nitrosyl species that are detected around 1870–1840 cm^{-1}. There is no agreement in the literature about the interpretation of this band and it has been assigned to mono- (Ni^{2+}-NO) (37–40) or to dinitrosyls ($Ni^{2+}(NO)_2$) (41, 42). At the same time adsorption of NO did not lead to formation of nitrosyls on the pure SiO_2 support (43), in agreement with the lack of Lewis acidity on silica (34). Introduction of 2.0 kPa NO to the IR cell causes the appearance of a band with a maximum at 1870 cm^{-1} which is assigned to nitrosyls of Ni^{2+} ions (37–42). This is in agreement with the results obtained by low-temperature CO adsorption. A similar behavior has recently been reported for Co^{2+} ions adsorbed on silica (43): they are not electrophilic enough to form carbonyls at room temperature and adsorbed CO is detected at low temperatures only. On the contrary, stable nitrosyls are formed at room temperature.

For the next experiments a sample of Ni–1–Si was reduced *in situ* at 973 K in flowing hydrogen. Adsorption of CO (1.6 kPa) on the sample thus treated produces an intense band with a maximum at 2050 cm^{-1}, a shoulder at 2078 cm^{-1}, and a weak band at 1922 cm^{-1} (Fig. 3, spectrum a), which evidences formation of carbonyls with the participation of metallic nickel (26, 29, 30). The 2050 cm^{-1} band initially increases in intensity with time and than starts to decline (Fig. 3, spectra b–d). After evacuation only two weak CO bands at 2060 and 1922 cm^{-1} remain in the spectrum (Fig. 3, spectrum e). Subsequent cycles of introduction of CO and evacuation result in the appearance and disappearance, respectively, of the 2050 and 2078 cm^{-1} bands: the intensity of the former band decreases with the number of cycles (Fig. 3, spectra f, g). In addition, in the gas phase a

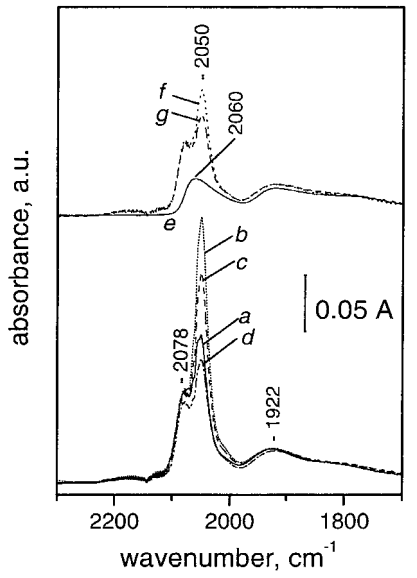

FIG. 3. FTIR spectra of CO adsorbed at ambient temperature on a Ni–1–Si sample *in situ* reduced at 973 K. Equilibrium CO pressures of 1.6 kPa (a) and evolution of the spectra in the CO atmosphere (b–d); evacuation (e); introduction of 1.6 kPa CO (f); subsequent evacuation and introduction of 1.6 kPa CO (g).

band at 2057 cm^{-1} assigned to gaseous nickel carbonyl (34) was detected. These results evidence that a loss of surface metal nickel occurs, as earlier reported for Ni/SiO_2 (34), Ni/TiO_2 (17), and Ni/ZrO_2 (18) systems.

The reduced sample was tested by CO at low temperature in order to check the eventual existence of residual Ni^{2+} ions. Adsorption of CO (200 Pa equilibrium pressure) at 85 K results in appearance of bands due to physically adsorbed CO (2138 cm^{-1}) and H-bonded CO (2157 cm^{-1}). The bands due to carbonyls of metallic nickel were visible below 2100 cm^{-1}. No bands assignable to Ni^{2+}–CO species were detected, which implies a full reduction of the nickel ions.

After the evacuation of CO, the sample was passivated by adding 200 Pa of O_2 into the IR cell at ambient temperature. After 5 min the oxygen was pumped out and the sample was tested by CO. No band of metal nickel carbonyls have been detected, which evidences that all of the surface situated Ni^0 atoms have been oxidized. Only a band at 2178 cm^{-1} with a very low intensity was detected. It disappeared after evacuation and is assigned to Ni^{2+}–CO carbonyls (3, 25–30), thus evidencing the existence, on the sample surface, of Ni^{2+} ions with a higher acidity than that of the initially adsorbed ions.

After CO evacuation, the sample was subjected again to oxidation; however, this time the interaction with oxygen was performed at 623 K. In order to detect all Ni^{2+} ions we performed the CO adsorption at low temperature. Introduction of CO (10 Pa) to the sample at 85 K (Fig. 4, spectrum a) resulted in the appearance of an asymmetric band at 2156 cm^{-1} (H-bonded CO) with a lower-frequency shoulder at 2138 cm^{-1} (physically adsorbed CO). Decreasing the equilibrium pressure/evacuation results in disappearance of the H-bonded and physically adsorbed CO and a Ni^{2+}–CO band at 2175 cm^{-1} is now clearly detected (Fig. 4, spectra d–g). The intensity of this band is lower than the intensity of the Ni^{2+}–CO band detected with the fresh Ni–1–Si sample. Taking into account that the CO extinction coefficient of σ-bonded and/or polarized CO weakly depends on the CO stretching frequency (37), it can be concluded that the number of accessible Ni^{2+} ions on the reoxidized sample is smaller than on the fresh one.

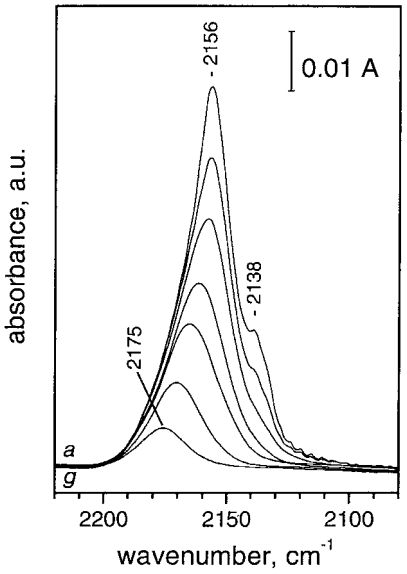

FIG. 4. FTIR spectra of CO adsorbed at 85 K on a Ni–1–Si sample *in situ* reduced at 973 K and reoxidized at 623 K. Equilibrium CO pressures of 10 Pa (a) and evolution of the spectra under dynamic vacuum (b–g).

These above results show that even at room temperature O_2 oxidizes all accessible Ni atoms to Ni^{2+} ions. Higher oxidation temperatures lead to an increase in concentration of these Ni^{2+} ions due to an additional oxidation of nickel from the metal particles and, most probably, to redispersion of the Ni^{2+} containing phase.

A Ni–2–Si sample was reduced *in situ* at 723 K. According to the TPR results, after this treatment all nickel deposited by the first procedure has to be in a metal state but no reduction of the nickel deposited by the second procedure is expected. The samples were tested by CO at 85 K. The results evidence a simultaneous existence on the sample surface of Ni^{2+} ions (band at 2193 cm^{-1} red shifted with increasing coverage) and metallic nickel (bands below 2100 cm^{-1}).

3.3. *X-ray Photoelectron Spectroscopy*

X-ray photoelectron spectroscopy is a convenient method of studying supported nickel catalysts (8, 12, 44, 45). The dispersion of the supported phase may be judged by the intensity of the Ni $2p_{3/2}$ peak, while the peak position is informative with respect to the oxidation state of nickel: metal nickel is characterized by a peak at about 853 eV, and peaks above this energy correspond to Ni^{2+} (44, 45). In addition, XPS can give information about the presence of a separate NiO phase which produces a doublet at about 853.5 and 855.5 eV (44).

The XPS spectra of the Ni/SiO_2 samples are presented in Fig. 5. The spectrum of Ni–1–Si exhibits a Ni $2p_{3/2}$ band at 857 eV, which is typical of Ni^{2+} ions (Fig. 5, spectrum a). The *ex situ* reduced Ni–1–Si sample also shows a Ni $2p_{3/2}$ band, however at lower energies, 856 eV (Fig. 5, spectrum b). In addition, the band is weaker in intensity and a careful study of the spectrum permits detecting a low-intensity shoulder at about 853 eV, which is characteristic of metallic nickel. These results show, in agreement with the results obtained by the other methods, that part of the metallic nickel has been oxidized after the contact of the sample with air. The lower intensity of the signal (related to the nonreduced sample) suggests a lower dispersion of nickel and is likely due to its redistribution in islands on the surface. The lower energy of the Ni $2p_{3/2}$ peak can be explained by the formation of a disperse two-dimensional "NiO"-like phase on the surface.

The spectrum of the *ex situ* reduced Ni–2–Si sample (Fig. 5, spectrum c) has a distinct peak of metallic nickel

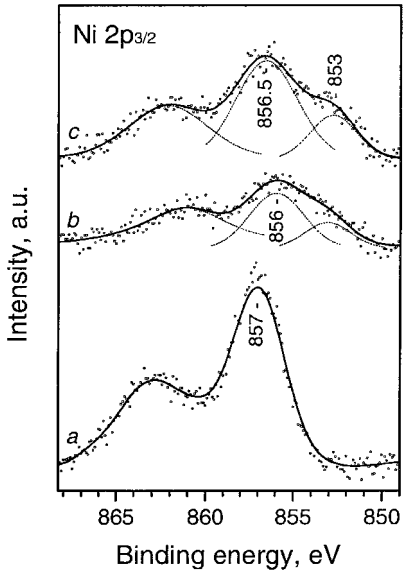

FIG. 5. XPS spectra of: Ni–1–Si (a), Ni–1–Si, *ex situ* reduced at 973 K (b) and Ni–2–Si *ex situ* reduced at 973 K (c).

(853 eV). The peaks of Ni^{2+} and Ni^0 are more intense than the respective peaks recorded with the reduced Ni–1–Si, which is due to an increase of the total nickel concentration. However, in contrast to sample Ni–1–Si (see spectrum a), the detected surface concentration of Ni^{2+} in the reduced Ni–2–Si sample is lower, which (when compared to the total nickel concentration) indicates a lower dispersion. The small difference between the Ni^{2+} peak positions (by 0.5 eV) in spectra "b" and "c" probably arises from the different Ni^{2+}/Ni^0 ratio in both samples.

3.4. Diffuse Reflectance UV-VIS Spectroscopy

To determine the initial state of the deposited nickel, the Ni–1–Si sample (ligh green in color) has been studied by electron spectroscopy. Its spectrum contains, in the 1300- to 300-nm region, four bands with maxima at 1080, 735, 660, and 400 nm (Fig. 6, spectrum a). These bands are typical of Ni^{2+} ions in octahedral surroundings and are due to the transitions $^3A_{2g} \rightarrow {}^3T_{2g}$ (1080 nm), $^3A_{2g} \rightarrow {}^3T_{1g}(F)$ (735 and 660 nm), and $^3A_{2g} \rightarrow {}^3T_{1g}(P)$ (400 nm) (46). The $^3A_{2g} \rightarrow {}^3T_{1g}(F)$ band is observed as a doublet due to the mixing of the close $^3T_{1g}$ and ^1E_g level states. The 660-nm band is more intense than that at 735 nm which proves weak exchange interaction between the nickel ions and indicates a high dispersion of the supported Ni^{2+} phase (46).

The spectrum of Ni–*i*–Si (grayish in color) manifests a high absorption background without distinct maxima (Fig. 6, spectrum b). This suggests the presence of Ni^{3+} ions (47) due to the formation (during the calcination) of a low-dispersed "NiO" phase having superstoichiometric oxygen in its structure.

3.5. Metal Particle Sizes

Metal particle size in the reduced Ni/SiO$_2$ samples has been determined by different techniques: XRD, TEM, and ferromagnetic resonance.

The XRD pattern of Ni–2–Si (*ex situ* reduced) contains a (111) nickel line with a half-width corresponding to a mean particle diameter of about 2 nm. Unfortunately, exact determination of the nickel particle size for Ni–1–Si sample has proved impossible by XRD because of the large half-width and the very low intensity of the line, but it seems that the metal particles on this sample are comparable to those on Ni–2–Si. In contrast, a rather sharp Ni (111) line has been detected in the diffraction pattern of the Ni–*i*–Si sample. Calculation has shown the mean metal particle diameter in this case to be 16 nm.

The Ni–1–Si and Ni–2–Si samples (*ex situ* reduced) have also been studied by TEM. The electron microscope photographs of Ni–2–Si show uniform nickel particles with a diameter of about 2–3 nm. Metal particles have not been noticed on the Ni–1–Si catalyst. This indicates that the Ni^0 particles in Ni–1–Si are probably smaller than those in Ni–2–Si.

Another technique giving information on the dispersion of supported ferromagnetic metals is FMR (48). The increase in metal particle size leads to an increase in the magnetization and the anisotropic effect. As a result, the resonance line broadens and the *g*-factor is shifted. It is still possible to detect a signal even with ferromagnetic particles having a diameter of dozens of nanometers. With very small particles ($d < 1$ nm) and low metal concentration the lines also become very broad and might not be detected.

The FMR spectra of Ni–1–Si and Ni–2–Si samples (*ex situ* reduced) show symmetric signals with a *g*-factor of 2.22

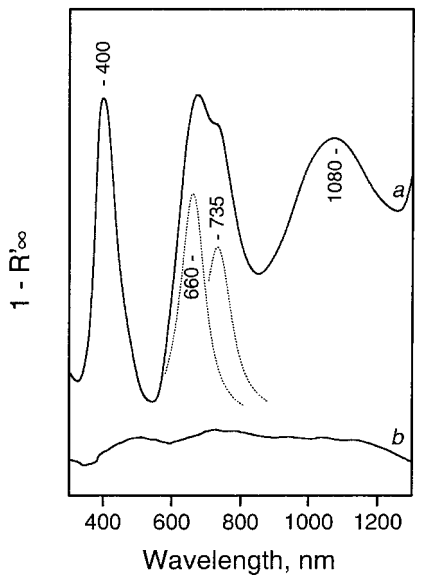

FIG. 6. DR UV–VIS spectra of Ni–1–Si (a) and Ni–*i*–Si (b).

and equal (within error limits) line widths, ΔH, of 300 G. The Ni–*i*–Si catalyst is characterized by a much wider line ($\Delta H = 1540$ G and $g = 2.35$), which is associated with much lower metal dispersion of Ni–*i*–Si than that seen with Ni–1–Si and Ni–2–Si.

3.6. Leaching Experiments

In order to establish whether some nickel from the reduced samples passes back into the solution when the next deposition procedure is performed, we carried out some leaching experiments. The reduced Ni–1–Si sample was subjected to a treatment similar to that used for the preparation of Ni–2–Si; however, ammonia (12.5 wt%) only was applied in this case. The result obtained showed that about 15% of the total nickel present in the sample had passed into the solution. Experiments were also performed by suspending silica in 12.5% ammonia solution at the same condition used for nickel deposition. No silica was detected to pass into the solution.

4. DISCUSSION

4.1. Nickel Ions on Silica

It is of interest to establish the mechanism of deposition of nickel cations on silica. Our results clearly prove that the process is not ion-exchange. In numerous studies it has been established that the ion-exchange on zeolites proceeds with the participation of the H^+ cations of the zeolite acidic surface hydroxyl groups (observed at ca. 3610 cm^{-1} in the IR spectra) but the terminal silanol groups are not involved in the reaction (35, 49). Accordingly, the spectra of our Ni–1–Si sample and SiO_2 do not differ from each other in the ν(OH) stretching region: in both cases terminal Si–OH groups at 3742 cm^{-1} have been detected. All this indicates that the deposition of nickel ions from amminocomplexes on silica is not an ion-exchange process. In general, the adsorption of cations on acidic oxide surfaces, such as SiO_2, proceeds at pH > ZPC (zero point charge) of the oxide (50). Under these conditions the adsorbed hydroxyl anions determine the negative surface charge and cations are adsorbed electrostatically in a second layer in order to preserve the neutral total charge. However, many cations (the so-called specifically adsorbed cations) are bound to the surface by additional forces. It has been found (51) that the double layer plays no decisive role in the adsorption of Ni^{2+} ions from nickel amminocomplex solutions on various oxides since the uptake coverage depends more strongly on the solution composition (determining the kind of the species being adsorbed) rather than the nature of the adsorbent. At the pH values used by us, the real adsorption species are expected to be $[Ni(NH_3)_5]^{2+}$ ions (51).

Since the Ni^{2+} ions on our sample are strongly bound to the surface (for instance they are not removed by washing) it is evident that silica has entered in the first coordination sphere of the nickel. The IR spectrum of Ni–1–Si in the region of OH stretching modes excludes the presence of a nickel hydroxide or nepoulite surface phase (characterized by OH bands at 3640 and 3645 cm^{-1}, respectively) and is rather similar to the IR spectrum of Ni/SiO_2 where the surface nickel silicates have the structure of talc (2). Indeed, it is reported in the literature that talc-type silicates are formed when the ion-exchange is performed at pH > 10 (2). The Si : Ni ratio in these silicates (2 : 1) is also consistent with the relatively low nickel concentration in our sample. We have no direct evidence of talc formation but similar structure is supported by the IR spectra of adsorbed CO. The relatively big chemical shift of CO evidences interaction between the adsorbed molecules through the solid. This may be explained by the fact that the nickel ions are placed in –O–Ni–O–Ni–O– rows, as in the talc structure. Note, however, that the Ni^{2+} ions are accessible for adsorption of probe molecules. This means that, if talc structure is formed, planes with exposed nickel are produced. There are data in the literature suggesting formation of talc structures where the nickel ions are sandwiched between two SiO_6-constituted layers (2). To obtain such a structure it is necessary to dissolve partially silica. Such a dissolution, however, can occur when the synthesis temperature is relatively high (ca. 370 K) and the contact time sufficiently long (at least several hours). Our experimental conditions are different and as a result the nickel ions on our sample are surface situated. It is possible, however, that negligible dissolution of silica has favored the formation of ordered structures.

One of the main conclusions to be drawn as a result of this study is that the properties of silica-supported nickel ions depend strongly on the sample synthesis method. The grafting leads to the formation of surface silicates (4, 8–10, 22, 52, 53) which are characterized by a high reduction temperature. The latter usually favors a large metal particle size. Irrespective of this, the characterization of the catalyst by various methods showed a high dispersion of the supported metal nickel. The impregnation method leads to less dispersed and inhomogeneously distributed Ni^{2+} as a "NiO"-like phase. Ni–*i*–Si can be reduced at a much lower (by 250 K) temperature than Ni–1–Si but the metal particles obtained after reduction are much larger.

4.2. Silica-Supported Metal Nickel

The metal particles on our Ni–1–Si sample are of high dispersion. This was observed by direct techniques, like TEM and XRD. However, the only information for the metal particles obtained *in situ* is by the IR spectra of adsorbed CO. Many data in the literature concerning CO adsorption on metallic nickel show that, in general, the adsorption forms at ambient temperature can be divided into two groups: (i) reversible and (ii) irreversible adsorption. The irreversible adsorption is also attributed to two different species: linear and bridged CO. If regular

crystal planes such as (100) and (110) are exposed on the metal surface (big nickel particles), the linear species are observed at ca. 2030 cm^{-1} (32). In addition, the bands due to bridged species (around 1900 cm^{-1}) are relatively intense. On the contrary, if the surface is "amorphous" (small metal particles) the bands due to linear species are more intense than the bands characterizing bridged species and are detected at higher frequencies (>2040 cm^{-1}) than the bands of CO linearly adsorbed on regular planes. With our sample the irreversibly adsorbed CO (Fig. 3, spectrum e) produced a band due to linear complexes at relatively high frequencies (2060 cm^{-1}) and was more intense than the band due to bridged CO. This clearly evidences that the "in situ" formed metallic nickel is highly dispersed.

Another set of bands arising after CO adsorption on nickel concerns the reversibly bound CO. There is agreement in the literature that these bands are typical of highly dispersed nickel (32–34). In our case these are the bands at 2078 and 2050 cm^{-1}. The first one is assigned to $Ni(CO)_x$ species ($x = 2$–3), whereas the latter band characterizes physically adsorbed $Ni(CO)_4$ (33, 34).

The Ni atoms formed during the reduction migrate to form metal particles. It is evident that this process liberates a free silica surface which can be used for the next deposition. If all of the nickel deposited during the second SDR procedure migrates during the reduction to the metal particles already formed with the participation of the nickel deposited by the first procedure, the latter should increase in diameter. This increase, however, should be very small (ca. 1.15 times). Unfortunately, we cannot draw definitive conclusions about such a small effect on the diameter of the metal particles. The easier reoxidation of nickel on the Ni–1–Si sample compared with the situation observed with the Ni–2–Si specimen suggest, however, formation of bigger metal particles in the latter case.

One of the main purposes of the present investigation is to establish to what extent the reoxidation of nickel affects the possibility of carrying out SDR. In principle, metal particles of higher dispersion are oxidized more easily. The results of the present paper show that a large part of metal nickel in the reduced Ni–1–Si catalyst is reoxidized even at room temperature when the sample is put in contact with oxygen (air). The IR spectroscopy data evidence that all accessible nickel atoms on the sample are oxidized to Ni^{2+}. This situation is different for Ni/TiO_2 and Ni/ZrO_2 samples prepared by SDR, where Ni^+ was found (17, 18).

The "NiO"-like phase obtained after oxidation of Ni^0/SiO_2 strongly differs in properties from surface nickel silicates. On the one hand, it is reduced at a much lower temperature and, on the other, the nickel ions in it have a more pronounced electrophilicity and are able to form complexes with CO at room temperature. It should be pointed out that this phase differs also from usual bulk NiO, as evidenced by TPR and XPS. The reduction temperature of reoxidized nickel ions depends on the temperature of the previous calcination of the samples. This is evidently associated with the dispersion of the "NiO" phase formed and is most probably due to the defects in the "NiO" structure. With rising reoxidation temperature the concentration of nickel ions detected by CO increases, which shows a higher oxidation degree and a higher surface concentration of Ni^{2+}.

It is evident that the reoxidation of nickel does not lead to migration of nickel ions to their initial location. This suggests that the main part of the silica surface liberated by reduction can again be active with respect to adsorption of Ni^{2+} ions. Indeed, the chemical analysis data show that the increase in nickel concentration after the second exchange is 1.53. A small part of the initially deposited nickel has passed into the solution during the second deposition and the real fraction of regenerated surface is larger. The remaining surface is physically blocked by metal nickel and "NiO"-like phase. The results presented in Table 1 demonstrate that SDR can be performed several times, although the amount of the deposited decreases with the number of SDR cycles.

On the basis of the results obtained one may propose the following scheme of Ni^{2+} SDR on SiO_2 (Fig. 7). The first deposition of Ni^{2+} ions results in formation of surface nickel silicates. Disperse metal particles are produced after reduction, while the major part of the active sites for deposition are liberated. After coming into contact with oxygen at room temperature, the nickel particles are covered by a layer consisting of a "NiO"-like phase which, however, remains localized around the metal particle. This allows a second deposition, as a result of which both, nickel silicates and metal nickel particles covered by a "NiO"-like phase, coexist on the sample surface. Reduction of this sample results in formation of metallic nickel particles with a mean diameter comparable with (and most probably little larger than) the particles formed on the reduced Ni–1–Si sample. At higher reoxidation temperatures (right hand side of Fig. 7) more metallic nickel is converted to "NiO"-like phase and the amount of surface Ni^{2+} ions increases.

5. CONCLUSIONS

- The Ni^{2+} ions deposited on SiO_2 by grafting from $Ni^{2+}(NH_3)_x$ solution possess a low acidity: they form complexes with CO only at low temperature. These nickel ions are characterized by a higher reduction temperature (TPR peak at 956 K) than the Ni^{2+} ions from the sample prepared by impregnation (two TPR peaks at 652 and 710 K).
- Highly dispersed (ca. 2 nm in diameter) metal particles are formed after reduction of the grafted Ni^{2+} cations. No regular crystal planes are exposed on their surface. As a result CO adsorption easily reacts with nickel forming volatile $Ni(CO)_4$ as a final product. The reduced sample prepared by impregnation (and having the same nickel concentration)

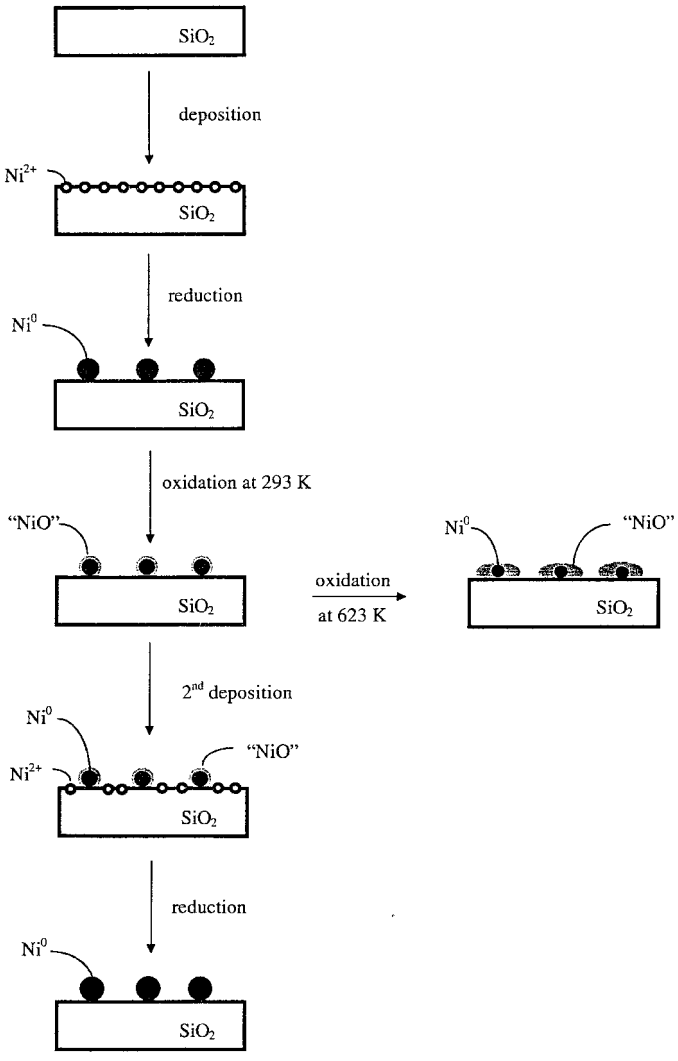

FIG. 7. Scheme of subsequent deposition–reduction (SDR) of Ni^{2+} ions on silica.

is characterized by much lower metal dispersion (main diameter of the nickel particles of 16 nm).

• The major part of the silica surface where the grafting proceeds is liberated after reduction of the Ni^{2+} cations and is not blocked again after exposure of the sample to oxygen (air). This permits subjecting the reduced sample to a second deposition and, as a result, the nickel concentration increases. Subsequent reduction results again in formation of highly dispersed nickel (main diameter of the metal particles ca. 2–3 nm).

• Subsequent deposition–reduction of Ni^{2+} ions on silica can be used to prepare highly dispersed nickel catalysts with different nickel concentrations.

ACKNOWLEDGMENTS

This work was supported by the Bulgarian National Research Foundation (Project X-486). K.H. acknowledges the award of an Alexander-von-Humboldt Fellowship and thanks Prof. H. Knözinger for providing the possibility to perform the FTIR experiments.

REFERENCES

1. Che, M., and Bennett, C. O., *Adv. Catal.* **38**, 55 (1989).
2. Kermarec, M., Carriat, J.-Y., Burattin, P., Che, M., and Decarreau, A., *J. Phys. Chem.* **98**, 12008 (1994).
3. Sault, A. G., Peden, C. H. F., and Boespflug, E. P., *J. Phys. Chem.* **98**, 1652 (1994).
4. Gil, A., Días, A., Gandía, L. M., and Montes, M., *Appl. Catal. A* **109**, 167 (1994).
5. Noh, J. S., and Schwarz, J. A., *J. Catal.* **127**, 22 (1991).
6. Hadjiivanov, K., Saint-Just, J., Che, M., Tatibouët, J.-M., Lamotte, J., and Lavalley, J.-C., *J. Chem. Soc. Faraday Trans.* **90**, 2277 (1994).
7. Lesage, P., Clause, O., Moral, P., Didillon, D., Candy, S. P., and Basset, J. M., *J. Catal.* **155**, 238 (1995).
8. Houalla, M., *Stud. Surf. Sci. Catal.* **3**, 273 (1982).
9. Burch, R., and Flamard, A. R., *Stud. Surf. Sci. Catal.* **16**, 311 (1982).
10. Burattin, P., Che, M., and Louis, C., *J. Phys. Chem. B* **101**, 7060 (1997).
11. Richardson, J. T., Dubus, R. J., Crump, J. G., Desai, P., Osterwalder, U., and Cale, T. S., *Stud. Surf. Sci. Catal.* **16**, 311 (1982).
12. Zakumbaeva, G., Zakharina, N., Beketaeva, L., and Naidin, V., *in* "Metal Catalysts" (D. V. Sokolsky, Ed.). Nauka, Alma-Ata, 1982.
13. Loosdrecht, J., van de, Kraan, A. M., van der, Dillen, A. J., van, and Geus, J. W., *J. Catal.* **170**, 217 (1997).
14. Afzal, M., and Theocharis, G. R., *Colloid Polym. Sci.* **271**, 1100 (1993).
15. Krall, V. C. H., Swaan, H. M., and Mirodatos, C., *J. Catal.* **161**, 409 (1996).
16. Hadjiivanov, K., Vassileva, E., Kantcheva, M., and Klissurski, D., *Mater. Chem. Phys.* **28**, 367 (1991).
17. Hadjiivanov, K., Mihaylov, M., Abadjieva, N., and Klissurski, D., *J. Chem. Soc. Faraday Trans.* **94**, 3711 (1998).
18. Mihaylov, M., Hadjiivanov, K., Abadjieva, N., Klissurski, D., and Mintchev, L., *Stud. Surf. Sci. Catal.* **118**, 295 (1998).
19. Haller, G. L., and Resasco, D. E., *Adv. Catal.* **36**, 173 (1989).
20. Mile, B., Stirling, D., Zammitt, M. A., Lovell, A., and Webb, M., *J. Catal.* **114**, 217 (1988).
21. Burattin, P., Che, M., and Louis, C., *J. Phys. Chem.* **102**, 2722 (1998).
22. Stiphaut, P. C. M., van, Doncer, H., Bayense, C. R., Geus, J. W., and Versluis, F., *Stud. Surf. Sci. Catal.* **31**, 55 (1987).
23. Louis, C., Cheng, Z. X., and Che, M., *J. Phys. Chem.* **97**, 5703 (1993).
24. Che, M., Cheng, Z. X., and Louis, C., *J. Am. Chem. Soc.* **117**, 2008 (1995).
25. Hadjiivanov, K., Klissurski, D., Kantcheva, M., and Davydov, A., *J. Chem. Soc. Faraday Trans.* **87**, 907 (1991).
26. Bonneviot, L., Cai, F. X., Che, M., Kermarec, M., Legendre, O., Lepetit, C., and Olivier, D., *J. Phys. Chem.* **91**, 5912 (1987).
27. Kasai, P. H., Bishop, R. J., Jr., and McLeod, D., Jr., *J. Phys. Chem.* **82**, 279 (1978).
28. Ione, K. G., Romannikov, V. N., Davydov, A. A., and Orlova, L. B., *J. Catal.* **57**, 126 (1979).
29. Peri, J. B., *Discuss. Faraday Soc.* **41**, 121 (1966).
30. Leglise, J., Janin, A., Lavalley, J.-C., and Cornet, D., *J. Catal.* **114**, 388 (1988).
31. Sheppard, N., and Nguyen, T. T., *Adv. IR Raman Spectrosc.* **5**, 67 (1978).
32. Zaki, M., *in* "Catalysis in Petroleum Refining and Petrochemical Industries" (M. Absi-Halabi *et al.*, Eds.), p. 569. Elsevier, Amsterdam, 1995.
33. Blacmond, D. G., and Ko, E. I., *J. Catal.* **96**, 210 (1985).
34. Martra, G., Swaan, H. M., Mirodatos, C., Kermarec, M., and Louis, C., *Stud. Surf. Sci. Catal.* **111**, 617 (1997).
35. Pieplu, T., Poignant, F., Vallet, A., Saussey, J., Lavalley, J.-C., and Mabilon, G., *Stud. Surf. Sci. Catal.* **96**, 619 (1995).

36. Beebe, T. P., Gelin, P., and Yates, J. T., Jr., *Surf. Sci.* **148**, 526 (1984).
37. Davydov, A., "IR Spectroscopy Applied to Surface Chemistry of Oxides." Nauka, Novosibirsk, 1984.
38. Atanasova, P., and Agudo, A. L., *Appl. Catal. B* **5**, 329 (1995).
39. Harrison, Ph., and Thornton, E., *J. Chem. Soc. Faraday Trans.* **74**, 2703 (1978).
40. Peri, J. B., *J. Catal.* **86**, 84 (1984).
41. Morrow, B. A., and Moran, L. E., *J. Catal.* **62**, 294 (1980).
42. Ouafi, D., Mauge, F., and Lavalley, J.-C., *Bull. Soc. Chim. Fr.* **28**, 363 (1989).
43. Djonev, B., Tsyntsarski, B., Klissurski, D., and Hadjiivanov, K., *J. Chem. Soc. Faraday Trans.* **93**, 4055 (1997).
44. Espinós, J. P., Gonzáles-Elipe, A. R., Fernández, A., and Munuera, G., *Surf. Interface Anal.* **19**, 508 (1992).
45. Sault, A. G., *J. Catal.* **156**, 154 (1995).
46. Reinen, D., *Ber. Bunsenges.* **69**, 82 (1965).
47. Propach, V., Reinen, D., Drenkhahn, H., Muller-Buschbaum, K., *Z. Naturforsch.* **33B**, 619 (1987).
48. Slinkin, A. A., *Usp. Khim.* **37**, 1521 (1968).
49. Fierro, G., Eberhardt, M. A., Houalla, M., Hercules, D. M., and Keith-Hall, W., *J. Phys. Chem.* **100**, 8568 (1996).
50. Brunnelle, J. P., *in* "Proceedings, Second International Symposium on the Preparation of Catalysts, Louvan-la-Neuve, 1978" (B. Delmon, P. Grange, P. Jacobbs, and G. Poncelet, Eds.), p. 211. Elsevier, Amsterdam, 1979.
51. Fuerstenau, D. M., and Osseo-Asare, K., *J. Colloid. Interface Sci.* **118**, 524 (1978).
52. De Lange, J. J., and Visser, G. H., *Ingenieur* **58**, 24 (1946).
53. Coenen, J. W. E., *Stud. Surf. Sci. Catal.* **3**, 89 (1979).